Graphitic carbon nitride embedded bio-based acrylic films as surface active photocatalysts

ACS Partner Journal

POLYMER SCIENCE & TECHNOLOGY

https://pubs.acs.org/PolySciTech

Letter

Graphitic Carbon Nitride Embedded Bio-Based Acrylic Films as Surface Active Photocatalysts

Chuyue Lu, Niklas Lorenz, Hanieh Bazyar,* Giulio Malucelli,* and Baris Kumru*

Cite This: *Polym. Sci. Technol.* 2025, 1, 46−52

Read Online

ABSTRACT: Soybean oil, a sustainable and renewable resource, has gained increasing industrial relevance through its derivatives, such as acrylated soybean oil, which is now produced at significant commercial scales. In contrast, graphitic carbon nitride (g-CN), a metal-free polymeric semiconductor, remains unexplored in industrial polymer systems. This study explores the integration of graphitic carbon nitride into bio-based acrylic resins using a rapid UV-curing process at a belt speed of 1 m/min. The resulting nanocomposite films, incorporating 10% nanoparticle loading and with an average thickness of 200 μm, demonstrate promising photocatalytic properties with a bandgap of 2.7 eV. The photocatalytic performance of these films is thoroughly evaluated via dye degradation experiments, revealing enhanced surface-driven activity, particularly in alcohol-based media. While the hydrophobic nature of the films limits dye removal in aqueous environments (25% removal efficiency in 5 h), complete photodegradation of methylene blue is achieved in alcohol within 5 h. Moreover, the films maintain their photocatalytic efficiency over five cycles with no significant performance deprivation.

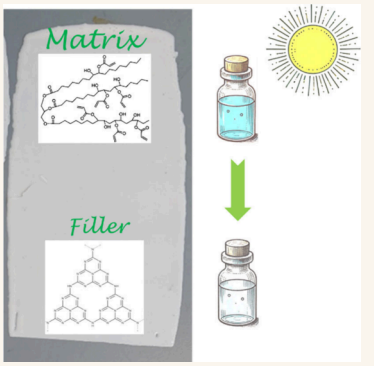

KEYWORDS: *photocatalytic films, renewable nanocomposites, functional coatings, carbon nitride dispersion, sustainable resins*

Water plays a crucial role in various industries, particularly in the textile sector, where it is integral to processes such as dyeing. However, the textile industry is one of the leading contributors to water pollution, significantly impacting environmental health.[1] Despite efforts to prevent waste, numerous water-soluble dyes, along with microplastics,[2] are discharged into the environment, posing significant threats to aquatic ecosystems and overall water quality.[3] Industrial dyes are categorized based on their chemical composition, with the chemical structure of each dye playing a pivotal role in determining its level of toxicity.[4] A case study involving two microalgae populations demonstrated that the cationic synthetic dye methylene blue (MB) significantly inhibits growth rates and disrupts chlorophyll production, ultimately reducing photosynthetic efficiency.[5] During metabolic digestion, the breakdown of these substances produces highly toxic byproducts, posing severe risks to both human and aquatic life.[6] Dye removal methods can be categorized into three groups based on their working mechanisms. Biological approaches utilize microorganisms and enzymes, employing either aerobic or anaerobic processes to transform toxic dyes into nontoxic byproducts.[7] Physical processes such as membrane filtration and adsorption stem from noncovalent interactions and size exclusion.[8] Chemical processes, such as advanced oxidation techniques like the Fenton reaction, effectively convert dye pollutants into nontoxic molecules.[9] Photocatalysis is an emerging technique for generating advanced oxidation products with high efficiency, excellent reusability, and reduced operational costs. While semiconductors are commonly used in colloidal form for dye removal processes,[10] they can present challenges in continuous operation modes due to issues with separation and mass transfer.

Polymeric coatings have become essential in a wide array of industries, spanning from maritime to aerospace, with most formulations primarily utilizing epoxy and acrylic chemistries.[11,12] The majority of coating formulations are based on petroleum-derived compounds; however, recent advancements are focused on increasing the incorporation of renewable materials into these formulations.[13] Soybean oil has been a key subject of research, and acrylated soybean oil is considered as a green coating material.[14] The functionality of coatings can be significantly enhanced by incorporating active agents and employing diverse chemical strategies, enabling the development of surfaces that possess anti-corrosive and self-healing properties.[15,16] Photoactive nanoparticles open up possibilities for creating surfaces capable of conducting photoredox-induced reactions under light illumination;[17] however, critical raw material-based formulations hamper sustainability. The use of metal-free polymeric semiconductor graphitic carbon nitride

Received: October 6, 2024
Revised: December 9, 2024
Accepted: December 17, 2024
Published: December 19, 2024

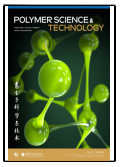

https://doi.org/10.1021/polymscitech.4c00017
Polym. Sci. Technol. 2025, 1, 46−52

(g-CN), characterized by its repeating tri-*s*-triazine structure, has been popularized in recent years.[18−20] g-CN has been documented for its role as a heterogeneous photocatalyst in photoredox-based reactions.[21−24] Its implementation into polymer networks has primarily been through aqueous dispersion and within porous structures like hydrogels.[25,26] For example, photoinduced waterborne coating recipe that combines 2-hydroxyethyl methacrylate with g-CN dispersion (2 wt % solid content in water-ethylene glycol), yields photoactive surfaces upon thermal curing at 120°C for static removal of Rhodamine B dye.[27] For broader applications, organomodified g-CN has been developed to facilitate integration into organic polymeric networks, such as poly(styrene-*co*-divinylbenzene) porous beads for the photocatalytic removal of Rhodamine B dye.[28] Recent innovations feature the integration of exfoliated thin g-CN nanosheets into custom-designed Schiff base coatings, developed as environmentally degradable antifouling surfaces.[29] Effective light penetration through the network is crucial for all light-induced reactions, which is why most studies prioritize the development of porous network structures.[30] Yet, the potential for integrating g-CN into nonporous industrial coating formulations and the properties of the resulting materials remain largely unexplored.

In the last decades, UV-curing has gathered remarkable scientific and industrial interest as an effective and reliable method suitable for manufacturing thermosetting polymeric materials as thin films or even thick components. Indeed, the possibility of avoiding the use of organic solvents (hence preventing the formation of VOCs (Volatile Organic Compounds) and therefore limiting the environmental impact), the high curing kinetics, and the low energy consumption (the energy is involved in the activation of the UV-curing process only) has justified the exploitation of this technique for different application sectors, ranging from optical fiber coatings, protective/multifunctional coatings, to printed circuit boards and printing inks, among others.[31−33] High radiation and temperature issues raised by Hg lamps can be quite easily limited by replacing high-pressure Hg lamps with light-emitting diodes (LEDs), moving from UV-curing to UV-LED curing.[34,35] This way, it is possible to increase energy saving through an improved electrical-to-optical conversion efficiency; besides, the absence of emission in the infrared wavelength region accounts for the delivery of cool radiation, suitable also for temperature-sensitive substrates.[36,37] Up to now, UV-LED curing has mainly been employed for the design and application of photocurable inks and coatings; however, only a few papers addressed investigating UV-LED curable nanocomposite systems. In this regard, Malucelli demonstrated the feasibility of the UV-LED curing process for the preparation of nanocomposite acrylic coatings containing 5 wt % of an organoclay and with enhanced thermal and barrier properties.[38] Wang and co-workers incorporated clay, talc, and calcium carbonate (filler loading around 50 wt %) into a UV-LED curable epoxy−acrylate resin formulation (with trimethylolpropane triacrylate as reactive diluent, and Ag nanoparticles) for designing thin coatings (75 μm thick) with enhanced wear resistance and antibacterial features against *S. aureus* and *E. coli*.[39] Then, the UV-LED curing was exploited to prepare poly(bisphenol-A-ethoxylate diacrylate) coatings containing phosphate glass powders at different loadings (from 10 to 50 wt %).[40] The incorporation of increasing amounts of filler significantly improved thermal and thermo-oxidative stability as well as demonstrated self-extinguishing properties in vertical flame spread tests. Furthermore, forced-combustion assessments revealed that coatings containing 50 wt % phosphate glass powders achieved a remarkable reduction in the peak heat release rate and total heat release by 44% and 33%, respectively, highlighting their effectiveness as smoke suppressants.

In this work, semiconducting graphitic carbon nitride particles will be dispersed in PureOmer 3005 resin with 10 wt % loading, and composite films will be manufactured via fast UV-LED curing setup that is rapid and scalable. Properties and photocatalytic activity of the so-formed films will be studied.

MATERIALS

A commercially available reactive epoxy soybean oil acrylate (PureOmer 3005, 84% bio-based content according to the ASTM D6866-21 standard) and 2,4,6-trimethylbenzoyl-diphenylphosphine oxide (herein after coded as TPO) were kindly supplied by IGM Resins (Mortara, Italy). Melamine was purchased from Alfa Aesar. 2,4-Diamino-6-phenyl-1,3,5-triazine, 4-methyl-5-vinylthiazole, benzoquinone, cyanuric acid, methylene blue (MB), methyl orange (MO) and *n*-hexane were obtained from Sigma-Aldrich. Solutions with water were prepared using pure water (Milli-Q grade) and using the Milli-Q IQ 7000 Ultrapure lab water system from Merck. Organomodified graphitic carbon nitride was synthesized from cyanuric acid and 2,4-diamino-6-phenyl-1,3,5-triazine complex as starting product as reported in literature[28] and cryomilled for 2 h to achieve smaller sizes for better dispersibility.

PREPARATION AND CURING OF THE UV-LED CURABLE FILMS

UV-LED thermoset cure process was adopted from our previous work[40] and schematically shown in Scheme S1. First, 4 wt % TPO (employed as photoinitiator) was dissolved in the PureOmer 3005 resin, heating the latter at 80°C for 20 min. Then, organic carbon nitride filler was added to the resin at 10 wt % loading; the optimal dispersion was achieved by mechanical stirring at room temperature for 30 min followed by 20 min ultrasonication. Then, the dispersions were coated on glass plates using a wire-wound applicator: the thickness of the obtained coatings was about 180 μm. Subsequently, the coated glass plates underwent the UV-LED curing process, using a Heraeus Noblelight UV-LED NC1 unit (Cambridge, UK), working in dynamic conditions (belt speed: 1 m/min), at 395 nm, with radiation intensity on the sample surface of about 4.8 W/cm^2. A single dynamic exposure under UV-LED radiation was sufficient to convert the liquid dispersions into the final cured composite film networks. Reference film was fabricated by following the same procedure without the addition of carbon nitride nanofillers. Details on characterization methods are presented in the Supporting Information.

Organomodified CN was synthesized as previously reported by our group,[28] which shows no special morphology and a diameter of around 300 nm, as evidenced by SEM and TEM (Figure S1). XRD profile of organomodified g-CN possesses characteristic (100) and (002) planes arising from in-plane and interplanar stacking, respectively (Figure S2).[41] DLS measurement shows nonuniform particle size distribution averaging on 750 nm (Figure S3); however, as measurement is conducted in aqueous dispersion, the exfoliation quality of organomodified

https://doi.org/10.1021/polymscitech.4c00017
Polym. Sci. Technol. 2025, 1, 46−52

g-CN is hindered. Following that, unfilled and CN filled films were fabricated (digital images are presented in Figure S4), as detailed in the experimental section. SEM images of top and side views of the filled film decipher homogeneous distribution of CN particles with small surface dents and minor agglomerates, with particle sizes larger than observed in TEM hinting toward low exfoliation capacity in acrylated soybean monomer (Figure 1A–C, Figure S5b). EDS analysis

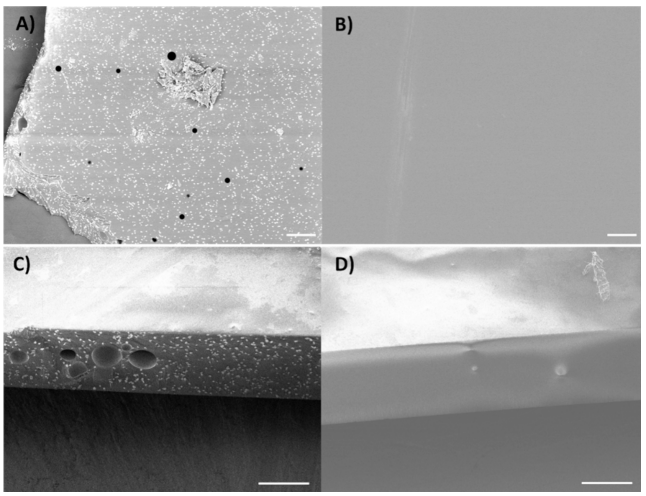

Figure 1. SEM images of filled (10 wt % g-CN) and unfilled acrylated soybean film: A) top view and C) side view of filled film; B) top view and D) side view of unfilled film (scale bars correspond to 100 μm).

proves carbon-, nitrogen-, and oxygen-based composition, whereas nitrogen and sulfur stem from carbon nitride incorporation (Figure S6). Such a hypothesis is proven by XPS measurement (Figure S7), and the existence of nitrogen and sulfur atoms on the sample surface arises from organo-modified carbon nitride nanoparticles. An AFM study is conducted to assess surface roughness, and a good surface finish with dents on the order of 500 nm is noted (Figure S8), indicating the efficacy of the UV-LED curing setup with no notable cure shrinkage. For the case of unfilled film, a defect-free homogeneous polymer layer is observed on top and side views (Figure 1B–D, Figure S5a). As these films are intended for coating use, no porosity is observed, as expected. While addition of nanofillers can prevent gelation efficiency in light-induced curing systems, it was not monitored in this case when 10 wt % organomodified g-CN nanofiller was employed. The gel content study shows almost 100% solid content, indicating full conversion of monomers within the film network (Table S1). However, higher loading of g-CN filler prevents gelation. Addition of g-CN nanofiller reduces water absorption compared to the reference film (0.74% versus 2.75%, Table S1), offering improved hydrolytic stability and fewer volumetric changes. Notably, g-CN proposes a notable stability against organic solvent uptake, as evidenced by swelling ratio comparison when *n*-hexane is used. Unfilled film has a tendency for *n*-hexane uptake with a swelling ratio of 34%; however, g-CN-based nanocomposite film exhibits 7.2%, concluding improved barrier properties in organic media.

Wettability measurements are essential for understanding and optimizing the surface properties of these materials. Static contact angle measurements directly indicate the strength of the interaction between the film surface and the liquid, reflecting the hydrophilic or hydrophobic nature of the surface. Figure 2A–D depicts the change of the static water contact angle on the filled film surface over 340 s, and Figure 2E shows the gradual decrease of the static water contact angle of both films. Filled film has a slightly higher water contact angle (84°) compared to the unfilled film (76°); hence, higher hydrophobicity is expected due to incorporation of organomodified g-CN nanofillers. Changes in WCA over time can be attributed to surface defects in the case of filled film and to minor swelling in the case of unfilled film. Advancing and receding angles contact angle (ARCA) measurements provide information on surface heterogeneity and the dynamics of expansion or contraction of the liquid on the surface. ARCA measurements indicate high hysteresis for both samples (Figure S9), but with notable hydrophobicity of the g-CN filled film compared to the unfilled film. g-CN filled film exposes higher hysteresis compared to unfilled film, and high hysteresis could be attributed to surface roughness, chemical composition of

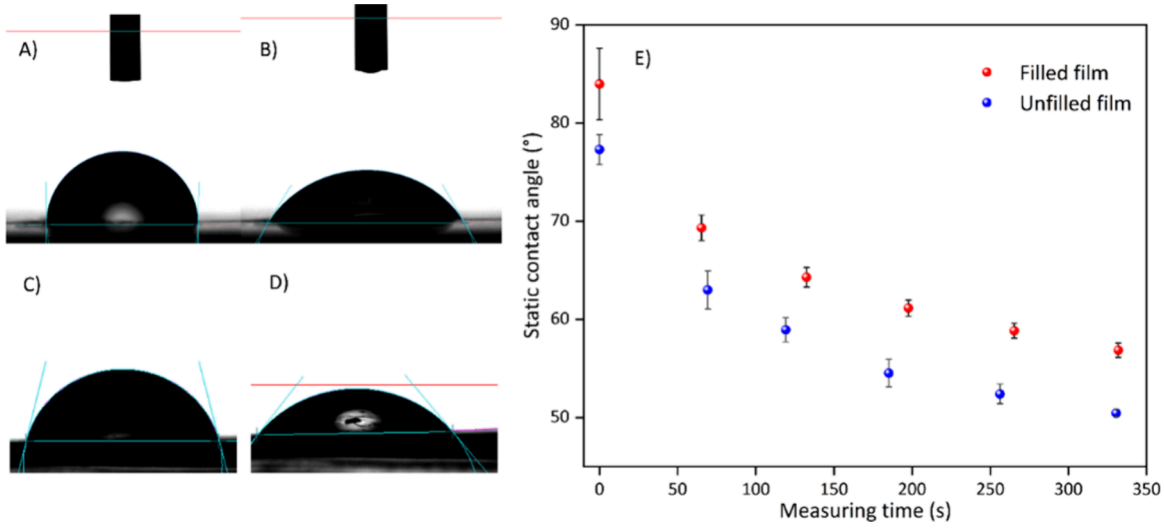

Figure 2. Variation of static contact angle with measurement time. A) Static contact angle of 10 wt % g-CN filled film at t = 0 s. B) Static contact angle of 10 wt % g-CN filled film at t = 340 s. C) Static contact angle of unfilled acrylated soybean film at t = 0 s. D) Static contact angle of unfilled acrylated soybean film at t = 340 s. E) Variation of static contact angle during the measurement time.

https://doi.org/10.1021/polymscitech.4c00017
Polym. Sci. Technol. 2025, 1, 46–52

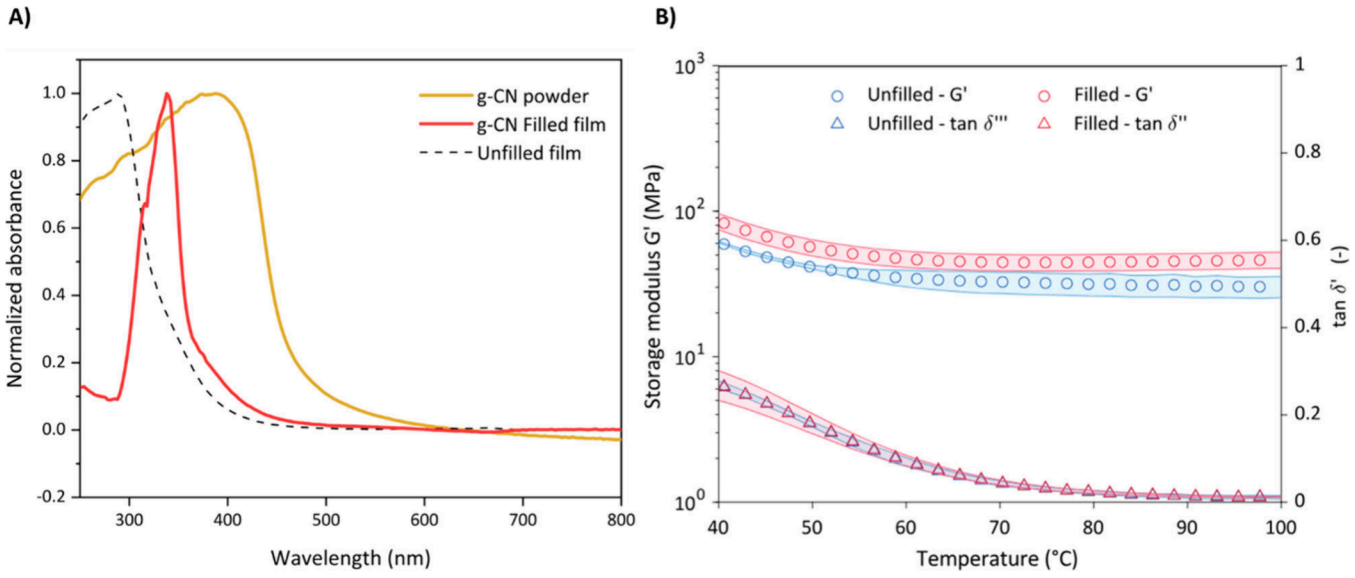

Figure 3. A) UV−vis spectrum of g-CN powder, 10 wt % g-CN filled film, and unfilled acrylated soybean film. B) Dynamic mechanical analysis of the 10 wt % g-CN filled and unfilled acrylated soybean film at rubbery state.

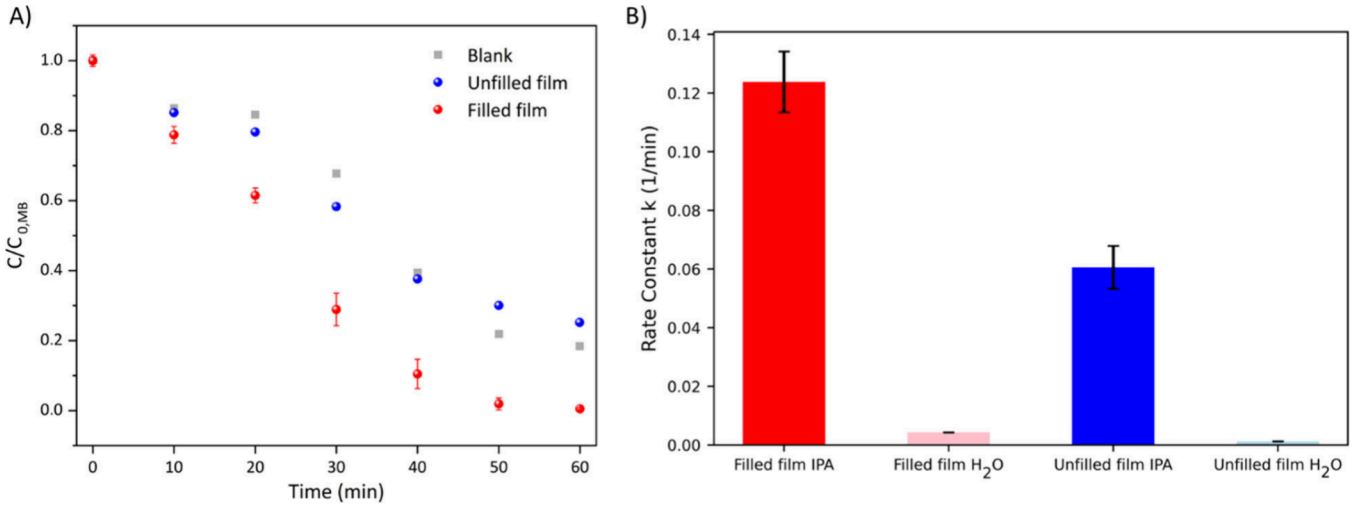

Figure 4. Static photocatalytic degradation of MB in 90% IPA. A) C/C_0 versus contact time of photocatalytic degradation of MB with linear regression. B) Rate constant comparison of degradation of MB in 90% IPA and in water.

surface and surface tension and viscosity of the subjected liquid.[42] In this case, surface heterogeneity during polymerization can render such a notable difference, as supported by AFM measurement in Figure S8.

Thermal stability of films is investigated by TGA (Figure S10), and high thermal stability up to 260 °C is observed for both samples. At 310 °C, decomposition begins and becomes pronounced at 400 °C. As g-CN has high thermal stability up to 600 °C,[43] and the mass difference at 550 °C corresponds to g-CN loading assuming the degradation of organic unfilled polymer film. The remaining mass from the filled film at higher temperatures can correspond to the formation of carbonaceous matter, as g-CN-polymer hybrids afford carbonized matter at elevated temperatures.[44] Optical properties are investigated via solid state UV−vis spectroscopy. g-CN powder has absorption in the visible range (Figure 3A) corresponding to a bandgap of 2.7 eV, as depicted by the Tauc plot in Figure S11. The unfilled film has a high optical transparency (Figure S4), as evidenced by UV−vis data in Figure 3A. The nanocomposite film has a sharp absorbance between 300 and 400 nm, indicating good activity in the UV range; however, to our surprise, it does not extend to a range as bare g-CN powder. Hence, photocatalytic studies are conducted under UV light, and almost no photocatalytic activity is observed under visible light when the reference experiment is conducted. The average values of three DMA measurements reveal a higher stiffness (25 %) of the filled film (Figure 3B). The rubbery storage modulus remains constant after the suggested glass transition below 40 °C for the investigated temperature range displaying the suggested operating temperatures. As so-formed coating is for intended use in film form; we believe that performing DMA measurement in the film state provides better accuracy. It is important to note that DMA results using films and nanocomposite films can significantly vary based on measurement conditions.[45]

Photocatalytic activity of the filled film is assessed by static dye degradation experiments. First, the importance of reaction media on the surface-driven photocatalytic process is

https://doi.org/10.1021/polymscitech.4c00017
Polym. Sci. Technol. 2025, 1, 46−52

monitored by using aqueous MB solution as a model pollutant. As the filled film possesses hydrophobicity and has no porosity, dye degradation performance in aqueous media is low. While the unfilled film reference exhibits minor self-degradation of MB (10%) under UV light in 90 min (Figure S12A–C), the filled film pushes degradation up to 32% (Figure S12B,C) as proven by improved degradation kinetics (Figure S12D). While this can be a noteworthy difference arising from the photocatalytic activity of the g-CN filled film, the values are considerably low for practical applications. Since PureOmer 3005 resin is intended for outdoor applications including alcohol as potential contact media, static dye degradation activity in 90% IPA solution is studied. It is known that IPA is detected in wastewater, especially arising from the solar cell industry.[46] Unlike photodegradation activity in water, the presence of IPA boosts degradation performance of the filled nanocomposite film (Figures S13 and S14).

While bare film also has an improved degradation rate compared to the aqueous system, the presence of g-CN clearly improves photocatalytic MB removal in IPA, as IPA acting as solvent transferring photoexcited charges more efficiently than the bulk surface. Figure 4A shows MB degradation, which clearly underlines enhanced removal efficiency of nanocomposite film following first-order kinetics, and Figure 4B summarizes dye degradation performance of filled and unfilled films in water and IPA reaction media. Despite the IPA acting as a hole scavenger, it renders a physical contact of dye onto the semiconductor embedded in the polymer matrix. Thus, one can hypothesize that dye degradation in this case proceeds via photogenerated electrons. To prove this assumption, a control experiment in the presence of benzoquinone as superoxide radical scavenger has been conducted.[47] As expected, no photocatalytic degradation is noted (Figure S15, a negligible decrease in absorption is due to self-degradation of MB). Potential dye degradation mechanism of MB employing a nanocomposite film is given in Scheme S1.

Nanocomposite film exhibits high reusability with a negligible decrease in MB photodegradation after 5 cycles in IPA (Figure 5), indicating dimensional stability and stable photocatalytic activity. Additionally, no leaching of g-CN particles has been observed. Dye degradation performance of films is examined in IPA using MO as a second model compound. Similarly, the unfilled film lacking photocatalytic function showed a minor degradation up to 19% due to self-degradation of MO (Figure S16); however, the filled film promotes MO degradation up to 57% under the same experimental conditions.

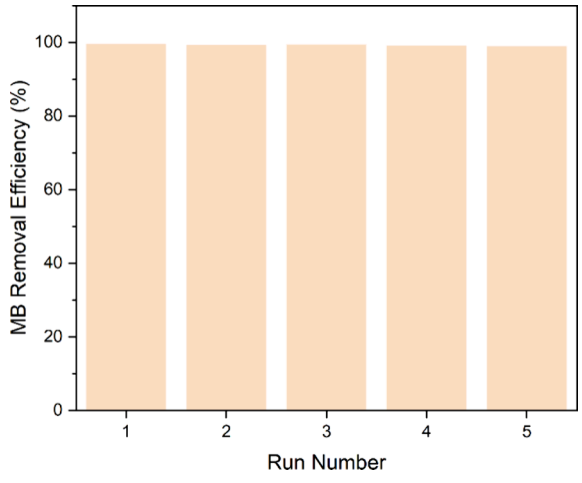

Figure 5. Reusability of 10 wt % g-CN filled films by means of photocatalytic static MB degradation (3 mg/L) exhibited on 5 consecutive runs.

The integration of fast-cure UV-LED technology presents a promising avenue for incorporating nanoparticle fillers into acrylic resin systems. In this study, we successfully incorporated graphitic carbon nitride (g-CN) nanoparticles into bio-based acrylic coatings using a fast-cure UV-LED process. This method enabled the incorporation of up to 10 wt % g-CN into polymer films without compromising gelation efficiency or causing cure shrinkage. Surface analysis confirmed the successful integration of g-CN. The resulting nanocomposite films demonstrate a significant reduction in water absorption (73% less), addressing a key limitation of bio-based resins. Moreover, the films exhibit enhanced resistance to organic solvents with 80% less swelling, improving their durability in organic environments. They also maintain thermal stability up to 260 °C. While the films' photocatalytic activity in aqueous media is limited due to their low water affinity, they exhibit improved photocatalytic performance in alcohol-based media. In the presence of alcohol, the photocatalytic degradation of methylene blue (at 3 mg/L concentration) occurs through excited electron transfer, achieving complete removal within 1 h under static conditions. Furthermore, the nanocomposite films retain high reusability, maintaining performance across five cycles, which significantly extends their operational lifespan. Obtained results suggest substantial potential for tailoring these bio-based acrylic coatings to meet the demands of specific industrial environments.

■ ASSOCIATED CONTENT

Supporting Information

The Supporting Information is available free of charge at https://pubs.acs.org/doi/10.1021/polymscitech.4c00017.

> Characterization methodology and details on photocatalytic experiments, analyses of g-CN powder, SEM images, XRD profile, DLS results, digital images of films, AFM data, particle size distribution and EDS, XPS spectra, gel content and swelling ratios, TGA, ARCA and reference photocatalytic experimental results, Tauc plot, UV–vis spectra, concentration vs degradation time, photographs of MB absorption, (PDF)

■ AUTHOR INFORMATION

Corresponding Authors

Hanieh Bazyar − *Faculty of Applied Sciences, Department of Chemical Engineering, Delft University of Technology, 2629 HZ Delft, Netherlands;* orcid.org/0000-0003-1689-9826; Email: h.bazyar@tudelft.nl

Giulio Malucelli − *Department of Applied Science and Technology, Politecnico di Torino, Alessandria 15121, Italy;* orcid.org/0000-0002-0459-7698; Email: giulio.malucelli@polito.it

Baris Kumru − *Faculty of Aerospace Engineering, Aerospace Structures & Materials Department, Delft University of Technology, 2629 HS Delft, Netherlands;* orcid.org/0000-0002-1203-4019; Email: b.kumru@tudelft.nl

https://doi.org/10.1021/polymscitech.4c00017
Polym. Sci. Technol. 2025, 1, 46−52

Authors

Chuyue Lu − *Faculty of Applied Sciences, Department of Chemical Engineering, Delft University of Technology, 2629 HZ Delft, Netherlands*

Niklas Lorenz − *Faculty of Aerospace Engineering, Aerospace Structures & Materials Department, Delft University of Technology, 2629 HS Delft, Netherlands;* orcid.org/0000-0003-1275-2579

Complete contact information is available at: https://pubs.acs.org/10.1021/polymscitech.4c00017

Notes

The authors declare no competing financial interest.

■ ACKNOWLEDGMENTS

B.K. and N.L. acknowledge funding from NEXTGEN HIGHTEC 01 GrowthFund program, and thank ASM department and DASML of Faculty of Aerospace Engineering of TU Delft.

■ REFERENCES

(1) Singh, B.J.; Chakraborty, A.; Sehgal, R. A systematic review of industrial wastewater management: Evaluating challenges and enablers. *J. Environ. Manage.* **2023**, *348*, No. 119230.

(2) Periyasamy, A.P.; Tehrani-Bagha, A. A review on microplastic emission from textile materials and its reduction techniques. *Polym. Degrad. Stab.* **2022**, *199*, No. 109901.

(3) Al-Tohamy, R.; Ali, S.S.; Li, F.; Okasha, K.M.; Mahmoud, Y.A.-G.; Elsamahy, T.; Jiao, H.; Fu, Y.; Sun, J. A critical review on the treatment of dye-containing wastewater: Ecotoxicological and health concerns of textile dyes and possible remediation approaches for environmental safety. *Ecotoxicol. Environ. Saf.* **2022**, *231*, No. 113160.

(4) Deblonde, T.; Cossu-Leguille, C.; Hartemann, P. Emerging pollutants in wastewater: A review of the literature. *Int. J. Hyg. Environ. Health* **2011**, *214*, 442−448.

(5) Krishna Moorthy, A.; Govindarajan Rathi, B.; Shukla, S. P.; Kumar, K.; Shree Bharti, V. Acute toxicity of textile dye Methylene blue on growth and metabolism of selected freshwater microalgae. *Environ. Toxicol. Pharmacol.* **2021**, *82*, No. 103552.

(6) Khan, I.; Saeed, K.; Zekker, I.; Zhang, B.; Hendi, A.H.; Ahmad, A.; Ahmad, S.; Zada, N.; Ahmad, H.; Shah, L.A.; Shah, T.; Khan, I. Review on Methylene Blue: Its Properties, Uses, Toxicity and Photodegradation. *Water* **2022**, *14*, 242.

(7) Ali, S.S.; Al-Tohamy, R.; Xie, R.; El-Sheekh, M.M.; Sun, J. Construction of a new lipase-and xylanase-producing oleaginous yeast consortium capable of reactive azo dye degradation and detoxification. *Bioresour. Technol.* **2020**, *313*, No. 123631.

(8) Santoso, E.; Ediati, R.; Kusumawati, Y.; Bahruji, H.; Sulistiono, D.O.; Prasetyoko, D. Review on recent advances of carbon based adsorbent for methylene blue removal from waste water. *Mater. Today Chem.* **2020**, *16*, No. 100233.

(9) Hoang, N.T.; Manh, T.D.; Nguyen, V.T.; Nga, N. T. T.; Mwazighe, F.M.; Nhi, B.D.; Hoang, H.Y.; Chang, S.W.; Chung, W.J.; Nguyen, D.D. Kinetic study on methylene blue removal from aqueous solution using UV/chlorine process and its combination with other advanced oxidation processes. *Chemosphere* **2022**, *308*, No. 136457.

(10) Houas, A.; Lachheb, H.; Ksibi, M.; Elaloui, E.; Guillard, C.; Herrmann, J.-M. Photocatalytic degradation pathway of methylene blue in water. *Appl. Catal. B: Environ.* **2001**, *31*, 145−157.

(11) Dyer, W.E.; Kumru, B. Polymers as Aerospace Structural Components: How to Reach Sustainability? *Macromol. Chem. Phys.* **2023**, *224*, No. 2300186.

(12) Zhang, T.; Zhang, T.; He, Y.; Wang, Y.; Bi, Y. Corrosion and aging of organic aviation coatings: A review. *Chin. J. Aeronaut.* **2023**, *36*, 1−35.

(13) Barroso, G.; Li, Q.; Bordia, R.K.; Motz, G. Polymeric and ceramic silicon-based coatings − a review. *J. Mater. Chem. A* **2019**, *7*, 1936−1963.

(14) Wu, Q.; Hu, Y.; Tang, J.; Zhang, J.; Wang, C.; Shang, Q.; Feng, G.; Liu, C.; Zhou, Y.; Lei, W. High-Performance Soybean-Oil-Based Epoxy Acrylate Resins: "Green" Synthesis and Application in UV-Curable Coatings. *ACS Sustainable Chem. Eng.* **2018**, *6*, 8340−8349.

(15) Beach, M.; Davey, T.; Subramanian, P.; Such, G. Self-healing organic coatings − Fundamental chemistry to commercial application. *Prog. Org. Coat.* **2023**, *183*, No. 107759.

(16) Chopra, I.; Ola, S.K.; Dhayal, P.V.; Shekawat, D.S. Recent advances in epoxy coatings for corrosion protection of steel: Experimental and modelling approach-A review. *Mater. Today Proc.* **2022**, *62*, 1658−1663.

(17) Crisenza, G. E. M.; Melchiorre, P. Chemistry glows green with photoredox catalysis. *Nat. Commun.* **2020**, *11*, 803.

(18) Li, H.; Zhu, B.; Cao, S.; Yu, J. Controlling defects in crystalline carbon nitride to optimize photocatalytic CO_2 reduction. *Chem. Commun.* **2020**, *56*, 5641−5644.

(19) Zhang, G.; Zhang, J.; Zhang, M.; Wang, X. Polycondensation of thiourea into carbon nitride semiconductors as visible light photocatalysts. *J. Mater. Chem.* **2012**, *22*, 8083−8091.

(20) Xiao, K.; Kumru, B.; Chen, L.; Jiang, L.; Schmidt, B. V. K. J.; Antonietti, M. A biomimetic nanofluidic diode based on surface-modified polymeric carbon nitride nanotubes. *Beilstein J. Nanotechnol.* **2019**, *10*, 1316−1323.

(21) Li, H.; Cheng, B.; Xu, J.; Yu, J.; Cao, S. Crystalline carbon nitrides for photocatalysis. *EES. Catal.* **2024**, *2*, 411−447.

(22) Barrio, J.; Li, J.; Shalom, M. Carbon Nitrides from Supramolecular Crystals: From Single Atoms to Heterojunctions and Advanced Photoelectrodes. *Chem.—Eur. J.* **2023**, *29*, No. e202302377.

(23) Teixeira, I.F.; Tarakina, N.V.; Silva, I.F.; Diab, G. A. A.; Salas, N.L.; Savateev, A.; Antonietti, M. Improving hydrogen production for carbon-nitride-based materials: crystallinity, cyanimide groups and alkali metals in solution working synergistically. *J. Mater. Chem. A* **2022**, *10*, 18156−18161.

(24) Teixeira, I.F.; Tarakina, N.V.; Silva, I.F.; Salas, N.L.; Savateev, A.; Antonietti, M. Overcoming Electron Transfer Efficiency Bottlenecks for Hydrogen Production in Highly Crystalline Carbon Nitride-Based Materials. *Adv. Sustain. Syst.* **2022**, *6*, No. 2100429.

(25) Lei, L.; Wang, W.; Wang, C.; Fan, H.; Yadav, A.K.; Hu, N.; Zhong, Q.; Mueller-Buschbaum, P. Hydrogel-supported graphitic carbon nitride nanosheets loaded with Pt atoms as a novel self-water-storage photocatalyst for H_2 evolution. *J. Mater. Chem. A* **2020**, *8*, 23812−23819.

(26) Hu, C.; Lin, Y.-R.; Yang, H.-C. Recent Developments in Graphitic Carbon Nitride Based Hydrogels as Photocatalysts. *ChemSusChem* **2019**, *12*, 1794−1806.

(27) Kumru, B.; Barrio, J.; Zhang, J.; Antonietti, M.; Shalom, M.; Schmidt, B. V. K. J. Robust carbon nitride-based thermoset coatings for surface modification and photochemistry. *ACS Appl. Mater. Interfaces* **2019**, *11*, 9462−9469.

(28) Esen, C.; Antonietti, M.; Kumru, B. Upgrading poly(styrene-co-divinylbenzene) beads: Incorporation of organomodified metal-free semiconductor graphitic carbon nitride through suspension photopolymerization to generate photoactive resins. *J. Appl. Polym. Sci.* **2021**, *138*, No. 50879.

(29) Wu, S.; Yan, M.; Wu, Y.; Wu, Y.; Lan, X.; Cheng, J.; Zhao, W. Designing a photocatalytic and self-renewed g-C3N4 nanosheet/poly-Schiff base composite coating towards long-term biofouling resistance. *Mater. Horiz.* **2024**, *11*, 4438−4453.

(30) Esen, C.; Kumru, B. Photocatalyst-Incorporated Cross-Linked Porous Polymer Networks. *Ind. Eng. Chem. Res.* **2022**, *61*, 10616−10630.

(31) Mendes-Felipe, C.; Oliveira, J.; Etxebarria, I.; Vilas-Vilela, J.L.; Lanceros-Mendez, S. State-of-the-art and future challenges of UV curable polymer-based smart materials for printing technologies. *Adv. Mater. Technol.* **2019**, *4*, No. 1800618.

(32) Wali, A.S.; Kumar, S.; Khan, D. A review on recent development and application of radiation curing. *Mater. Today Proc.* **2023**, *82*, 68−74.
(33) Patil, R.S.; Thomas, J.; Patil, M.; John, J. To Shed Light on the UV Curable Coating Technology: Current State of the Art and Perspectives. *J. Compos. Sci.* **2023**, *7*, 513.
(34) Liu, S.; Borjigin, T.; Schmitt, M.; Morlet-Savary, F.; Xiao, P.; Lalevee, J. High-Performance Photoinitiating Systems for LED-Induced Photopolymerization. *Polymers* **2023**, *15*, 342.
(35) Schmitz, C.; Poplata, T.; Feilen, A.; Strehmel, B. Radiation crosslinking of pigmented coating material by UV LEDs enabling depth curing and preventing oxygen inhibition. *Prog. Org. Coat.* **2020**, *144*, No. 105663.
(36) Dreyer, C.; Motoc, D.L.; Koehler, M.; Goldenberg, L. UV LED Curable Perfluoropolyether (PFPE)-Urethane Methacrylate Transparent Coatings for Photonic Applications: Synthesis and Characterization. *Polymers* **2023**, *15*, 2983.
(37) Appelhoff, L.; Hornemann, N.; Schmidt, J.; Krautz, A.; Strehmel, B. Combination of NIR and UV-LEDs enables physical and chemical drying of aqueous coating dispersions as new green technology. *Appl. Res.* **2024**, *3*, No. e202400011.
(38) Malucelli, G. Synthesis and characterization of UV-LED curable nanocomposite coatings. *Curr. Org. Chem.* **2017**, *21*, 2314−2321.
(39) Wang, X.; Feng, Y.; Zhang, L.; Protsak, I.; Jamali, R.; Shu, Y.; Pal, P.; Wang, Z.; Yang, J.; Zhang, D. Fast-cured UV-LED polymer materials filled with high mineral contents as wear-resistant, antibacterial coatings. *Chem. Eng. J.* **2020**, *382*, No. 122927.
(40) Pugliese, D.; Malucelli, G. UV-LED Curable Acrylic Films Containing Phosphate Glass Powder: Effect of the Filler Loading on the Thermal, Optical, Mechanical and Flame Retardant Properties. *Polymers* **2022**, *14*, 1899.
(41) Yao, Y.; Wang, Y.; Lu, T.; Zhang, J.; Hu, K.; Zhang, H.; Pukala, T.; Liu, Y.; Duan, X.; Wang, S. In-plane implanting carbon rings into carbon nitride to intrigue nonradical photodegradation. *Appl. Catal. B: Environ.* **2024**, *342*, No. 123363.
(42) Extrand, C.W.; Kumagai, Y. An experimental study of contact angle hysteresis. *J. Colloid. Interface Sci.* **1997**, *191*, 378−383.
(43) Esen, C.; Antonietti, M.; Kumru, B. Oxidative Photopolymerization of 3,4- Ethylenedioxythiophene (EDOT) via Graphitic Carbon Nitride: A Modular Toolbox for Attaining PEDOT. *ChemPhotoChem.* **2021**, *5*, 857−862.
(44) Esen, C.; Kumru, B. Thiol-ene polymer beads via liquid−liquid printing: armored interfaces and photopolymerization via graphitic carbon nitride. *Nanoscale Adv.* **2022**, *4*, 3136−3141.
(45) Deng, S.; Hou, M.; Ye, L. Temperature-dependent elastic moduli of epoxies measured by DMA and their correlations to mechanical testing data. *Polym. Test.* **2007**, *26*, 803−813.
(46) Xiao, Y.; Xu, H.-Y.; Xie, H.-M.; Yang, Z.-H.; Zeng, G.-M. Comparison of the treatment for isopropyl alcohol wastewater from silicon solar cell industry using SBR and SBBR. *Int. J. Environ. Sci. Technol.* **2015**, *12*, 2381−2388.
(47) Shah, J.H.; Fiaz, M.; Athar, M.; Ali, J.; Rubab, M.; Mehmood, R.; Jamil, S. U. U.; Djellabi, R. Facile synthesis of N/B double-doped Mn_2O_3 and WO_3 nanoparticles for dye degradation under visible light. *Environ. Technol.* **2020**, *41*, 2372−2381.

https://doi.org/10.1021/polymscitech.4c00017
Polym. Sci. Technol. 2025, 1, 46−52